12

Discrete Wavelet Transform Application to the Protection of Electrical Power System: A Solution Approach for Detecting and Locating Faults in FACTS Environment

Enrique Reyes-Archundia, Edgar L. Moreno-Goytia,
José Antonio Gutiérrez-Gnecchi and Francisco Rivas-Dávalos
Instituto Tecnológico de Morelia, Morelia, Michoacán, México

1. Introduction

The Wavelet Transform has been widely used to process signals in engineering and sciences areas. This acceptance is rooted on its proven capability to analyze fast transients signals which is difficult to perform with the FFT. In the area of electrical engineering, a number of publications have been presented about the analysis of phenomena in electrical grid at medium and high voltage levels. Some solutions have focused on the power quality (Chia-Hung&Chia-Hao, 2006; Tse, 2006), short-term load forecasting (Chen, 2010) and protection of power systems (Kashyap&Shenoy, 2003; Ning&Gao, 2009). However, there are few contributions in the open literature focusing in using WT for implementing relaying protection algorithms in power grids with presence of FACTS. The Thyristor Controlled Series Capacitor (TCSC), the Universal Power Flow Controller (UPFC), the Static Synchronous Series Compensator (SSSC), and the Statcom are some of the power controllers developed under the umbrella name of "Flexible AC Transmission Systems" (FACTS). These devices play a key role in nowadays electrical networks because they have the capability of improving the operation and control of power networks (power transfer, transient stability among others characteristics). Collateral to their many strong points, the FACTS controllers also have secondary effects on the grid that should be taken into account for engineering the next generation of protection schemes.

In power grids, -transmission lines included-, there are three-phase, two-phase and single-phase fault events. At fault occurrence of any type, a fast transient signal, named travelling wave-, is produced and propagates through the power lines. The travelling waves are helpful in determining the fault location in such line, faster than using other methods, if the appropriate tools are used.

This chapter presents the application of the Discrete Wavelet Transform (DWT) for extracting information from the travelling waves in transmission line and separate such waves from the signals associated to the TCSC and SSSC. This signal discrimination is useful to improve protections algorithms.

The chapter also presents a brief description of DWT in section 2 and includes a review of FACTS controllers in section 3. Section 4 presents the procedure to separate the effects of power electronic controller. Finally, sections 5 and 6 present the system under test and the results in locating faults in power lines.

2. Wavelet Transform

The Wavelet Transform (WT) is a tool highly precise for analyzing transient signal. The WT is obtained from the convolution of the signal under analysis, $f(t)$, with a wavelet Ψ, both related to the coefficients C as shown in (1)

$$C(scale, position) = \int_{-\infty}^{\infty} f(t)\Psi(scale, position, t)dt \tag{1}$$

where Ψ is the "mother" wavelet, is so named because it belongs a "family" of special wavelets to compare with $f(t)$. Examples of wavelets families are: Haar, Daubechies, Symlets, Mexican Hat, Meyer, Discrete Meyer. Ψ is selected to analyze a unknown portion of signal using convolution, i.e. the wavelet transform can detect if the analyzed signal is closely correlated with Ψ under a determined scale and position.

The WT produces a time-scale space. In the wavelet context, "scaling" means "stretching" or "compressing" a signal, as shown if fig. 1. In this way, scaling is related to frequency, meaning this that the smaller the scale factor, the more "compressed" the wavelet, i.e. smaller scale factors are corresponding with high frequencies.

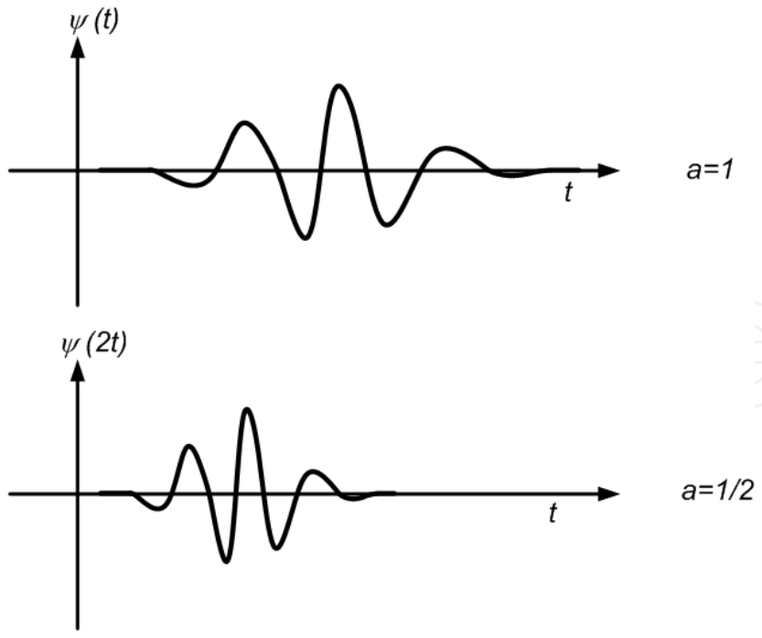

Fig. 1. Scaling the wavelet signal

In the other hand, the term "position" is referred to shifting the wavelet, this is delaying or advancing the signal, as shown if fig 2. $\psi(t-\tau)$ is delayed τ seconds of $\psi(t)$.

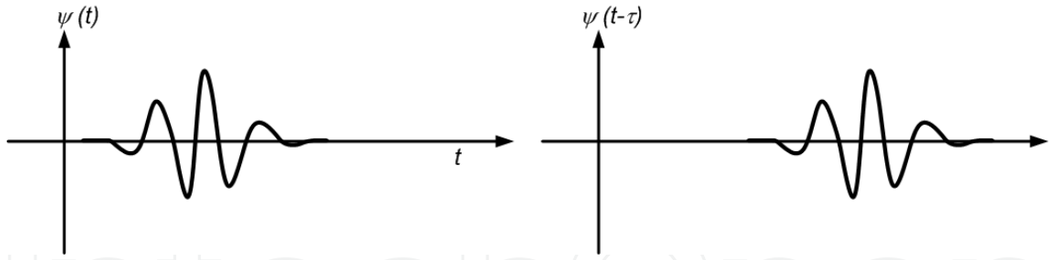

Fig. 2. Shifting the wavelet signal

Due to the easiness to modify the scale-position parameters, the wavelet analysis enables (Misiti, 2001):

1. The use of long time intervals where more precise low-frequency information is needed
2. Shorter regions where high-frequency information is needed.
3. To perform local analysis, that is, to analyze a localized area of a larger signal.

If a subset of scales and positions is taken under consideration instead a large number of coefficients then the analysis can be performed more efficiently. Scales and positions based on power of 2 (known as dyadic) are the common selection. The analysis performed under the aforementioned consideration is named Discrete Wavelet Transform (DWT), because is referred to discrete values.

In the DWT process, the input signal is filtered and sampled down. This processing keeps all valuable information complete but reduces the number of data needed. Two data sequences are obtained once the procedure is perform: Approximations (*cA*n) and Details (*cD*n). The former are the high-scale, low-frequency components of the signal and latter are the low-scale, high-frequency components. Both correspond to DTW coefficients, as shown in fig. 3. After filtering the signal is left down sampled but keeping complete information

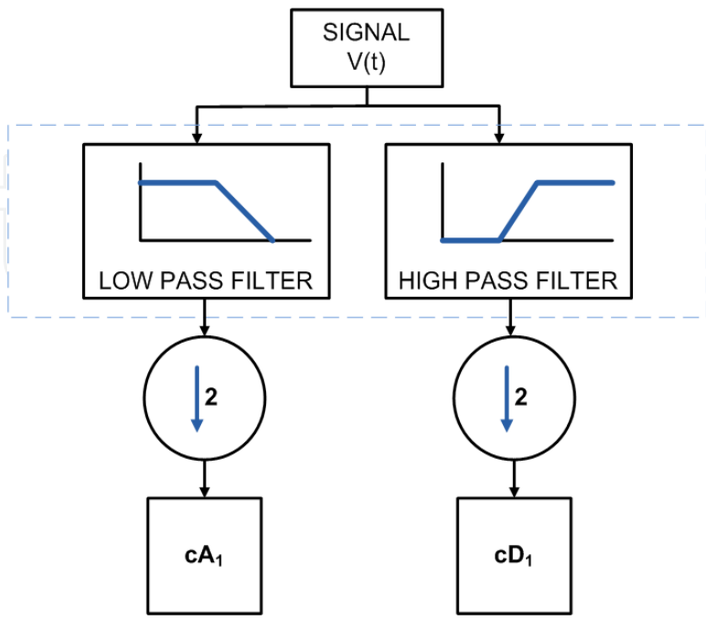

Fig. 3. Discrete Wavelet Transform

cA_1 and cD_1 are obtained by (2) (Misiti et. al. 2001)

$$cA_1(t) = \sum_k f(t).L_d(k-2t)$$
$$cD_1(t) = \sum_k f(t).H_d(k-2t) \quad (2)$$

where cA_1, is the approximation coefficient of level 1, cD_1 is the detail coefficient of level 1. L_d is the low-pass filter and H_d is the high-pass filter. These filters are related to mother wavelet ψ. In this process, signal $f(t)$ is divided in two sequences, cD_1 contains highest frequency components ($f_s/4$ to $f_s/2$ range, where f_s equals sampling frequency of $f(t)$) and cA_1 lower frequencies (lower than $f_s/4$). At this stage, cD_1 extract elements of $f(t)$ in $f_s/4$ to $f_s/2$ range that maintains correlation with ψ.

As aforesaid, the initial decomposition of signal $f(t)$ is the level 1 for Approximations (cA_1) and Details (cD_1). This cA_1 can in turn be divided in two sequences of Approximations and Details and then a new level of decomposition is obtained (cA_2 and cD_2). This procedure is repeated until the required level for the application is reached, as shown in fig. 4.

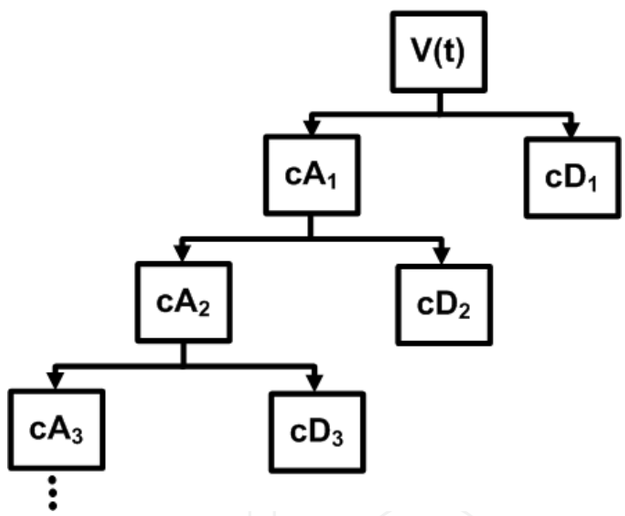

Fig. 4. Wavelet decomposition tree.

Of course, cA_2 and cD_2 are obtained from cA_1 after to pass a filter and sampling down stage. In this way, sequences cD_1, cD_2, … cD_n relates $f(t)$ to ψ at different scales, i.e. different frequency ranges. (2) can be extended for higher levels cD and cA, as shown in (3)

$$cA_{n+1}(t) = \sum_k cA_n(t).L_d(k-2t)$$
$$cD_{n+1}(t) = \sum_k cA_n.H_d(k-2t) \quad (3)$$

3. Flexible AC Transmission Systems (FACTS)

In this section, a brief description of series and shunt FACTS controllers is presented with emphasis on the TCSC and SSSC.

The FACTS controllers, once installed in the power grid, helps to improve the power transfer capability of long transmission lines and the system performance in general. Some of the benefits of the FACTS controllers on the electric system:

1. Fast voltage regulation,
2. Increased power transfer over long AC lines,
3. Damping of active power oscillations, and
4. Load flow control in meshed systems,

The FACTS controllers are commonly divided in 4 groups (Hingorani&Gyugyi, 2000):

1. Series Controller. These controllers are series connected to a power line. These controllers have an impact on the power flow and voltage profile. Examples of these controllers are the SSSC and TCSC.
2. Shunt Controllers. These controllers are shunt connected and are designed to inject current into the system at the point of connection. An example of these controllers is the Static Synchronous Compensator (STATCOM).
3. Series-shunt controllers. These controllers are a combination of serial and shunt controllers. This combination is capable of injecting current and voltage. An example of these controllers is the Unified Power Flow Controller (UPFC).
4. Series-series controllers. These controllers can be a combination of separate series controllers in a multiline transmission system, or it can be a single controller in a single line. An example of such devices is the Interline Power Flow Controller (IPFC)

The STATCOM, the TCSC and the SSCC are three of the FACTS controllers highlighted by their capacity to provide a wide range of solutions for both normal and abnormal conditions. Figures 5 to 7 illustrates the STATCOM, TCSC and SSSC structures and its network connection.

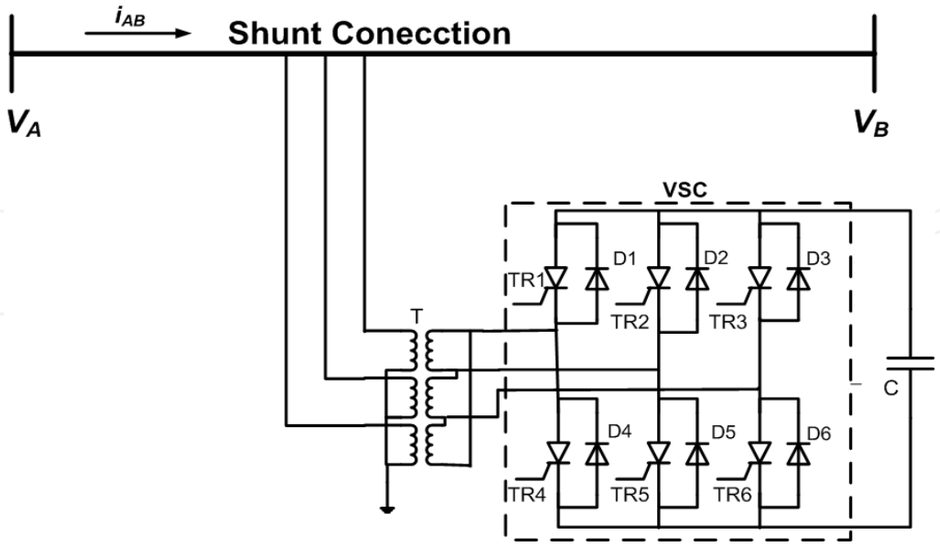

Fig. 5. STATCOM

The STATCOM is a voltage-source converter (VSC) based controller which maintains the bus voltage by injecting an ac current through a transformer.

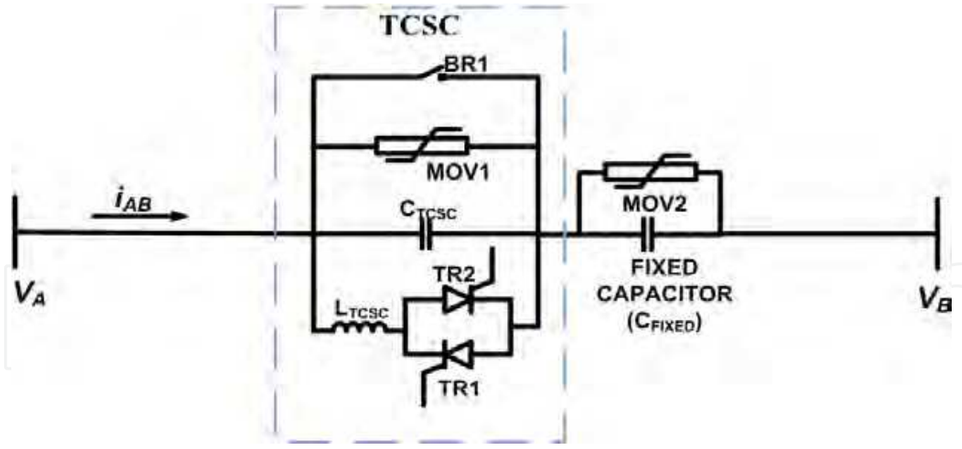

Fig. 6. TCSC

The TCSC is made of a series capacitor (C_{TCSC}) shunted by a thyristor module in series with an inductor (L_{TCSC}). An external fixed capacitor (C_{FIXED}) provides additional series compensating. The structure shown in fig. 4 behaves as variable impedance fully dependable of the firing angle of the thyristors into the range from 180° to 90°. Normally the TCSC operates as a variable capacitor, firing the thyristor between 180° to 150°. The steady state impedance of TCSC (X_{TCSC}) is (4)

$$X_{TCSC}(\alpha) = \frac{X_{CTCSC} X_{LTCSC}(\alpha)}{X_{LTCSC}(\alpha) - X_{CTCSC}} \tag{4}$$

Where

$$X_{LTCSC}(\alpha) = X_{LTCSC} \frac{\pi}{\pi - 2\alpha - \sin\alpha}, X_{LTCSC} < X_{LTCSC}(\alpha) \leq \infty$$

where α is the firing angle of thyristor.

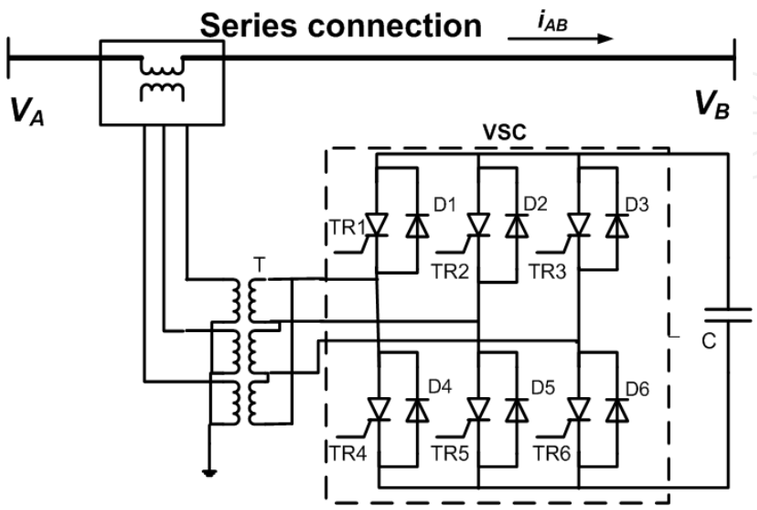

Fig. 7. SSSC

The SSSC injects a voltage in series with the transmission line in quadrature with the line current. The SSSC increases or decreases the voltage across the line, and thereby, for controlling the transmitted power.

3.1 FACTS effects on conventional protection schemes

The transmission lines are commonly protected with a distance protection relay. A key element for this protection is the equivalent impedance measured from the relay to the fault location, as shown on fig. 8. In non-compensated lines, the distance to the fault is lineally related to this impedance.

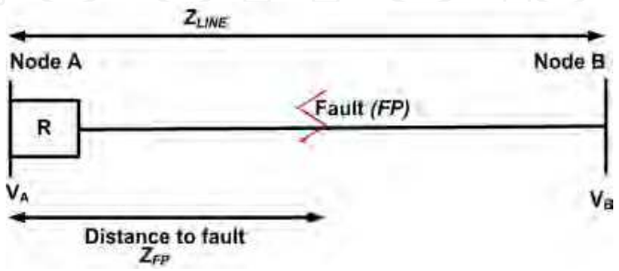

Fig. 8. Distance Relay

Before the fault occurs, the relay (R) measures voltage and current at node A and calculate the total impedance of line (Z_{LINE}). When fault occurs at fault point (*FP*), the impedance measured by R is lower than Z_{LINE} ($Z_{FP} < Z_{LINE}$) and proportional to distance between *FP* and node A.

In transmission lines compensated with series FACTS such impedance, -from measuring point of reference-, presents a nonlinear behavior. The impedance can abruptly change depending on the location of the fault in the line, after or before the FACTS controller. As mentioned above, protection relays for no compensated power lines centers its operation in a linear relationship between the distance to the fault and the equivalent impedance. For instance, the collateral effects of STATCOM on impedance had been presented in some detail (Kazemi et.al., 2005; Zhou et.al., 2005) showing that the shunt controller produces a modification in tripping characteristics for relay of protection. The impedance variation induced by the STATCOM affects the distance protection, meaning this that the fault is not precisely located in the line and the distant to the fault is wrongly determined. In relation with the UPFC, some studies indicate that this controller have significant effects on the grid at the point of common coupling, PCC, greater than those from shunt-connected controller (Khederzadeh, 2008). Similarly, series-connected FACTS controllers tends to reduce the total equivalent impedance a transmission line. As the conventional distance protection relies on the linear equivalent impedance-fault distance relationship, at fault occurrence such protection, -installed at in one end of the line-, faces two scenarios: a) scenario 1: the fault is located between the protection and the series FACTS, and b) scenario 2: the fault is not located between the protection and the series FACTS but after the controller. As example, Figure 9 shows the effect of the TCSC on the equivalent line impedance. It can be notice in Fig. 9 (b) that TCSC reduces the electrical line length, which means a reduction of the total equivalent impedance. In this case, a conventional distance protection can detect and locate a fault for the scenario 1 (a) but wrongly operates for scenario 2 (b).

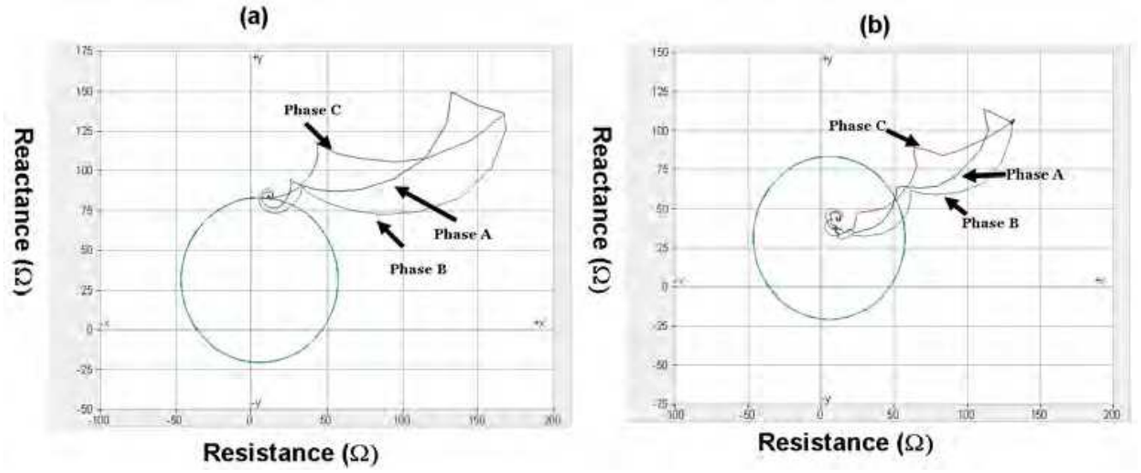

Fig. 9. Impedance of a transmission line after a three-phase fault at the end of line, a) without TCSC, b) with TCSC

The aforementioned nonlinear behavior is caused by the relationship $Z_{LINE\_COMP} = Z_{LINE} - Z_{TCSC}$. In the fault scenario 1 $Z_{LINE\_COMP} = Z_{LINE}$; but in the fault scenario 2 $Z_{LINE\_COMP} = Z_{LINE} - Z_{TCSC}$. Fig. 10 shows the nonlinear relation. The TCSC is situated at the middle of the line.

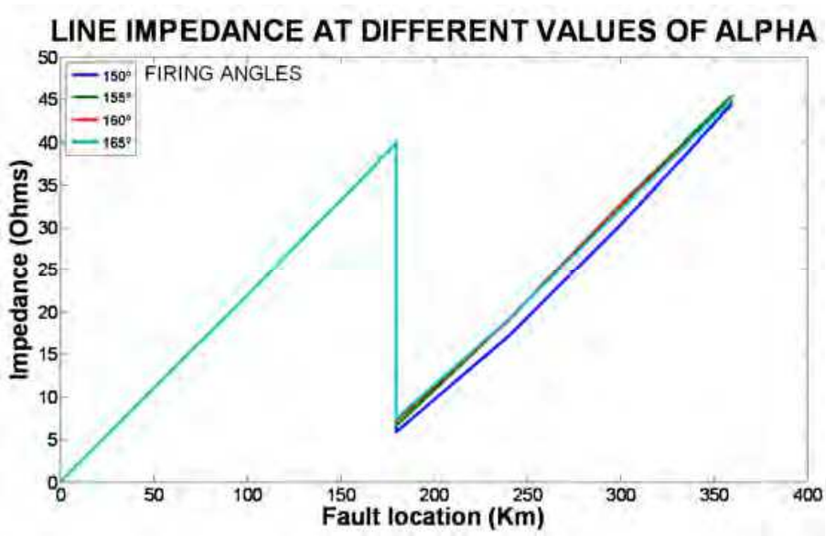

Fig. 10. Line impedance with TCSC after a fault.

As figure 10 shows, if the fault occurs before the TCSC location impedance has a linear relationship with distance to fault, however when fault occurs after the position of FACTS, then the impedance suffers a non linear change, evidenced by reduction of impedance, that cause a malfunction on distance relay.

4. Procedure to detect and locate faults

As shown in section 3, in compensated grid such the conventional distance protection schemes face conditions not taken into account in its original design, therefore the next

generation of protection installed should include algorithms with built-in techniques to deal with the particularities of grids in a FACTS context.

Artificial intelligence and digital signal processing techniques, DSP, have both provided a sort of tools to power systems engineers. In particular the combination of wavelets with artificial intelligence and estimation techniques is an attractive option for analyzing electrical grids in the current context.

In order to deal with the impedance nonlinear variation characteristic associated to the series FACTS compensation, various solutions have been proposed in the last decade. One of these proposals uses traveling waves to detect and locate faults in a transmission line (Shehab-Eldin&McLaren, 1988). As is known, after a fault in a transmission line two traveling waves are produced, this is shown if figure 11(a). The traveling wave is used to detect and locate the fault. The latter is achieved determining the time the wave needs to travel from the fault position *(FP)* to the measurement point (M_1). Fig. 11(b), illustrates a lattice diagram of traveling waves. After the fault, the wave needs a time t_1 to travel from *FP* to M_1. When the traveling wave reach a point at which impedance is different to characteristic impedance (Z_0), then the wave is reflected, because of that, the wave is reflected when reach the node *A* and returns to *FP*. Once the wave reaches *FP* is reflected because the impedance at *FP* is different to Z_0 and travels again to node *A* in a time equals to t_2. The fault is detected at time t_1 and time elapsed between t_1 and t_2 is useful to locate the fault position. This is possible because t_2-t_1 has a linear relationship with distance to fault.

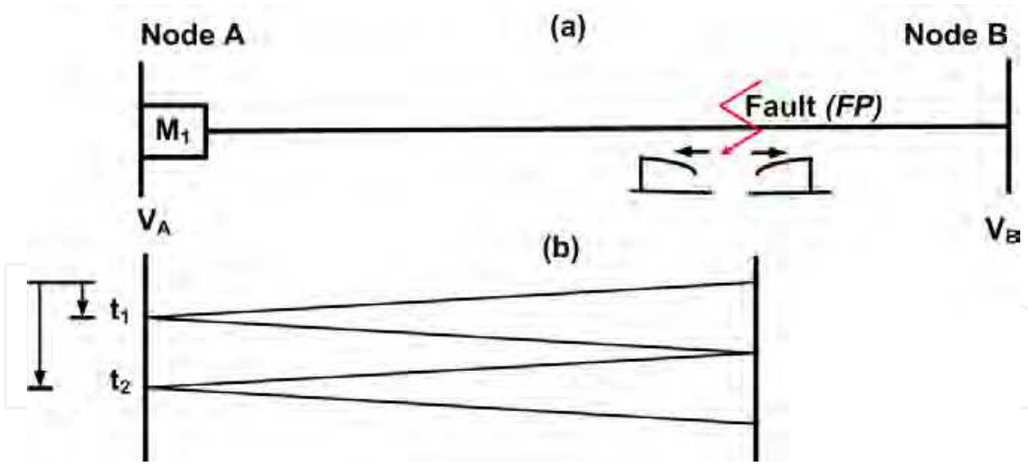

Fig. 11. a) Traveling waves in a faulted line; b) Laticce diagram

It's important to analyze the effects caused by FACTS on traveling wave to determine if this latter can be used to detect and locate faults at FACTS environment. Considering a controller installed at the middle of the line, if fault occurs before the position of FACTS, as illustrated in fig. 12(a), the traveling wave can be analyzed at the same way that without controller, because it don´t encounter points of different impedance to Z_0 between *FP* and M_1. In the other hand, if fault occurs after the position of controller, as shown in Fig. 12(b), the wave encounters the FACTS when traveling from *FP* to M_1.

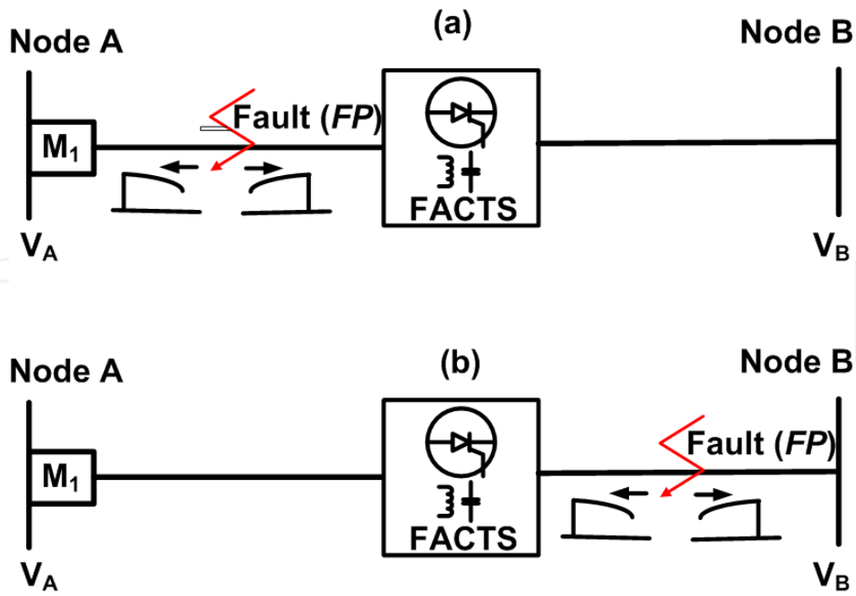

Fig. 12. Travelling waves generated after a fault at FACTS environment

The aim of subsections 4.1 and 4.2 is to show that traveling waves can be used to detect and locate faults when FACTS are installed. To demonstrate the neutrality of some series-connected FACTS on travelling waves, the TCSC and the SSSC are analyzed. Once the wave reaches the FACTS controller, two characteristics are evaluated: a) the effect of FACTS on magnitude of traveling wave, b) the harmonics due to FACTS.

The above are based on two hypotheses: a) the magnitude of traveling wave is not significantly affected when crossing FACTS because this latter doesn't contribute greatly to make different the impedance at location of controller to Z_0 and wave is not reflected at this point; b) the main harmonics of FACTS are the 3th , 5th and 7th (Daneshpooy&Gole, 2001; Sen, 1998), and discrete wavelet transform to analyze traveling wave can be adjusted to separate the harmonics from FACTS of signal due to fault, through proper selection of coefficient of detail.

4.1 Effects on the magnitude of traveling waves

To demonstrate that magnitude of traveling wave is not greatly affected when crossing the FACTS is necessary to analyze the coefficient of reflection (ρ_v) at the FACTS location. ρ_v indicates the energy of traveling wave that is reflected when reach the controller position. If impedance at FACTS location is different to Z_0 then the wave is reflected otherwise there is not reflection.

The voltage equation in any x point along the line for long lines is given by (Pourahmadi-Nakhli&Zafavi, 2011)

$$v_x = (V_- e^{-\gamma x} + V_+ e^{\gamma x}) \tag{5}$$

$$\gamma^2 = \alpha + j\beta = \sqrt{(R + j\omega L)(G + j\omega C)}$$

where α is the attenuation constant , β is phase constant and γ is a propagation constant. $V_+e^{+\gamma x}$ represents wave traveling in negative direction and $V_- e^{-\gamma x}$ represents wave traveling in positive direction at x point (considering x=0 at node A), as shown in fig. 13.

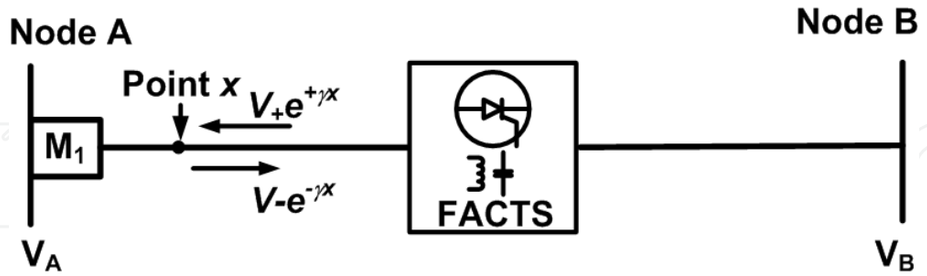

Fig. 13. Voltage in any point along the line

If Z_x (the impedance at x point) is different to Z_0, there is a coefficient of reflection (ρ_v) given by (6),

$$\rho_v = \frac{Z_x - Z_0}{Z_x + Z_0} \tag{6}$$

4.1.1 Travelling waves and the TCSC

Considering x point matches with FACTS location, then impedance at this point is given by contribution of Z_0 and impedance of TCSC. Fig. 14 illustrates the TCSC scheme under study and table 1 shows its parameters.

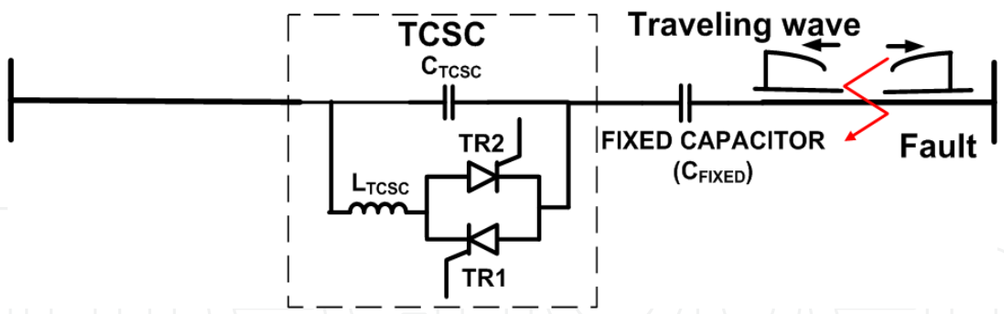

Fig. 14. TCSC controller

Parameter	Value
Line voltage, infinite bus	400 kV
Line length	360 km
C_{TCSC}	95 μF
L_{TCSC}	8.77 mH
Cfixed	98 μF
Z_0 (considering a lossless line)	550 Ω

Table 1. Electric Parameters

When the travelling wave reaches the thyristor, this can be open or closed. If the thyristor is open at the moment when the wave reaches it, the array seen by wave is as shown in fig. 15.

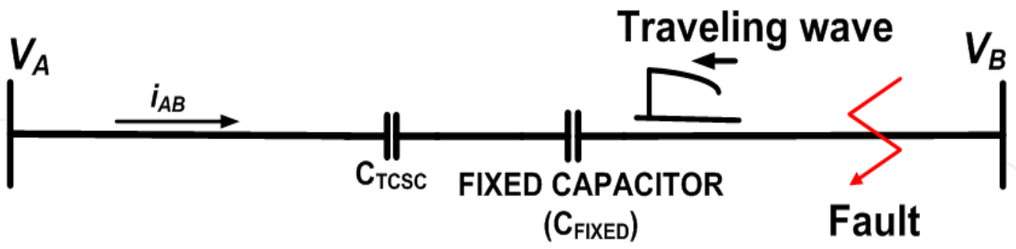

Fig. 15. Traveling wave when Thyristor is open

From fig. 11, the impedance at FACTS location is given by (7)

$$Z_x(s) = Z_0 + \frac{1}{sC_{TCSC}} + \frac{1}{sC_{FIXED}} = Z_0 + \frac{C_{TCSC} + C_{FIXED}}{s(C_{TCSC})(C_{FIXED})} \tag{7}$$

The coefficient of reflection seen at discontinuity is obtained by substituting (7) in (6)

$$\rho_v = \frac{\frac{C_{TCSC} + C_{FIXED}}{sC_{TCSC}C_{FIXED}}}{2Z_0 + \frac{C_{TCSC} + C_{FIXED}}{sC_{TCSC}C_{FIXED}}} = \frac{\frac{1}{sC_{SERIE}}}{2Z_0 + \frac{1}{sC_{SERIE}}} = \frac{1}{s2Z_0C_{SERIE} + 1} \tag{8}$$

where $C_{SERIE} = (C_{TCSC}) \| (C_{FIXED})$.

Because the capacitor opposes to abrupt changes in voltage, the wave tends to pass through the TCSC without a significant decrement. From (6), the voltage decreases with a constant time given by $\tau = 2Z_0C_{SERIE}$

> If C_{TCSC} = 98μF, C_{FIXED} = 95 μF, and Z_0 = 550 Ω, then τ = 53.1 ms. This array needs 212.2 ms to discharge; however, the traveling wave makes the travel in 1.2 ms, so the discontinuity due to TCSC represents only a decrement of 0.6% in magnitude of front of voltage wave.

If thyristor is closed at the moment when the wave reaches it, the array seen by wave is as shown in fig. 16.

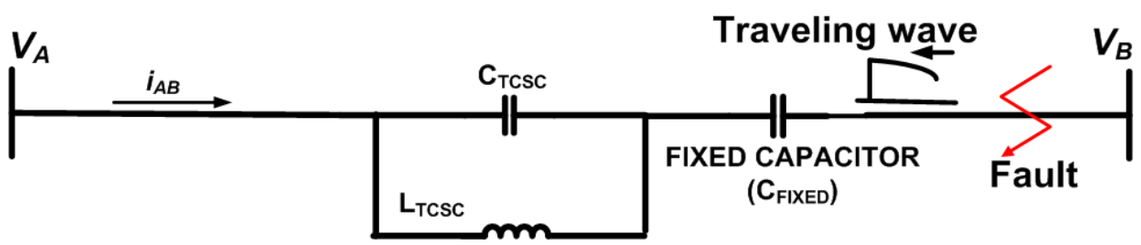

Fig. 16. Traveling wave when Thyristor is closed

From fig. 16, the impedance seen at this point is given by (9)

$$Z_x(s) = Z_0 + \frac{1}{sC_{FIXED}} + \frac{\frac{1}{sC_{TCSC}} sL_{TCSC}}{\frac{1}{sC_{TCSC}} + sL_{TCSC}} \tag{9}$$

ρ_v is obtained by substituting (9) in (6)

$$\rho_v = \frac{\frac{1}{sC_{FIXED}} + \frac{\frac{1}{sC_{TCSC}} sL_{TCSC}}{\frac{1}{sC_{TCSC}} + sL_{TCSC}}}{2Z_0 + \frac{1}{sC_{FIXED}} + \frac{\frac{1}{sC_{TCSC}} sL_{TCSC}}{\frac{1}{sC_{TCSC}} + sL_{TCSC}}} = \frac{\frac{1}{sC_{FIXED}} + \frac{sL_{TCSC}}{1+s^2L_{TCSC}C_{TCSC}}}{2Z_0 + \frac{1}{sC_{FIXED}} + \frac{sL_{TCSC}}{1+s^2L_{TCSC}C_{TCSC}}}$$

$$\rho_v = \frac{1 + s^2L_{TCSC}C_{TCSC} + s^2L_{TCSC}C_{FIXED}}{2Z_0(1+s^2L_{TCSC}C_{TCSC})sC_{FIXED} + 1 + s^2L_{TCSC}C_{TCSC} + s^2L_{TCSC}C_{FIXED}} \tag{10}$$

$$\rho_v = \frac{s^2(L_{TCSC}C_{TCSC} + L_{TCSC}C_{FIXED}) + 1}{s^3 2Z_0 L_{TCSC}C_{TCSC}C_{FIXED} + s^2(L_{TCSC}C_{TCSC} + L_{TCSC}C_{FIXED}) + s2Z_0C_{FIXED} + 1}$$

In this case, L_{TCSC}= 8.8 mH, so the constant time of decrease is τ = 107.5 ms, and 430.1ms are needed to reflect the wave. As the wave need 1.2 ms. to travel along the line, no significant decrease is done.

4.1.2 Travelling waves and the SSSC

An SSSC can emulate a series-connected compensating reactance and is represented by a voltage source (Vq) in series with reactance of coupling transformer (X_L) (Sen, 1998). The Fig. 17 pictures the SSSC equivalent circuit.

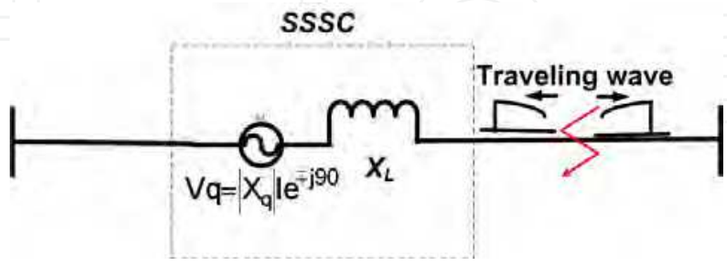

Fig. 17. SSSC Controller

Once the wave reaches the SSSC, the impedance seen by wave is (11)

$$Z_x(s) = Z_0 + jX_L \tag{11}$$

ρ_v is obtained substituting (11) in (6)

$$\rho_v = \frac{jX_L}{jX_L + 2Z_0} \tag{12}$$

Due the transformer was selected to work as a coupling instrument, X_L is enough small to give a ρ_v near to zero. So, the magnitude of incident wave is no significantly affected by SSSC. In the present case $X_L = wL = (2\pi)(60)(0.1\text{mH}) = 0.0377\ \Omega$ and $Z_0 = 550\ \Omega$, then

$$\rho_v = \frac{0.0377j}{0.0377j + 2(550)} \approx \frac{0.0377j}{1100} \approx 0$$

Because of the value of ρ_v is zero and then there is not reflection of wave when reach the position of SSSC, so the magnitude of traveling wave is not affected.

In the case of both controllers, TCSC and SSSC, is evidenced that the magnitude of traveling waves are unaffected when passing through the FACTS controller and they are not an obstacle for the travelling waves to be a good option to detect and locate faults.

4.2 FACTS harmonics effects on WT

Although magnitude of traveling wave is no significantly affected by TCSC, a proper coefficient of detail in wavelet transform is needed to be selected. This is because the wavelet transform can detect the harmonics due to FACTS. This frequency can mix up with the traveling waves at some coefficients of details reason why is important to identify. For instance, the main harmonics of TCSC are 3th and 5th (Daneshpooy&Gole, 2001)

Table 2 shows the frequency ranges of the coefficients of details for the signals under analysis. The above considering a sampling frequency of 10 kHz. It can be seen that cD_5, correspond to 156-312 Hz range, so main harmonics of TCSC are placed in that level.

Level of Coefficient of Detail	Range of frequency
cD1 (level 1)	2500 Hz to 5 kHz
cD2 (level 2)	1250 Hz to 2500 Hz
cD3 (level 3)	625 Hz to 1250 Hz
cD4 (level 4)	312.5 Hz to 625 Hz
cD5 (level 5)	156 Hz to 312 Hz

Table 2. Range of frequency with coefficient of detail

As example to show the above, a three phase to ground fault is simulated at 300 km from M_1, as illustrated in fig. 18. The fault occurs at 0.3 s. Two cases are considered: a) without FACTS and b) with FACTS.

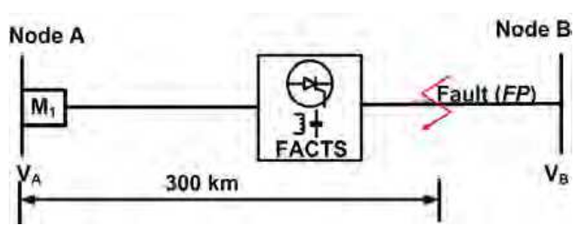

Fig. 18. Three phase to ground fault at 300 km.

Because the fault is simulated after the position of controller, the voltage measurement in M_1, contains harmonics induced by FACTS. To analyze the range of frequency at which fault signal and harmonics of FACTS are present, (3) is used to calculate cD_n of voltage obtained from M_1. Five coefficients of detail are considered because harmonics due to TCSC are present at range 156-312 Hz (see table 2). The results obtained when the fault is simulated with and without FACTS are presented in fig. 19

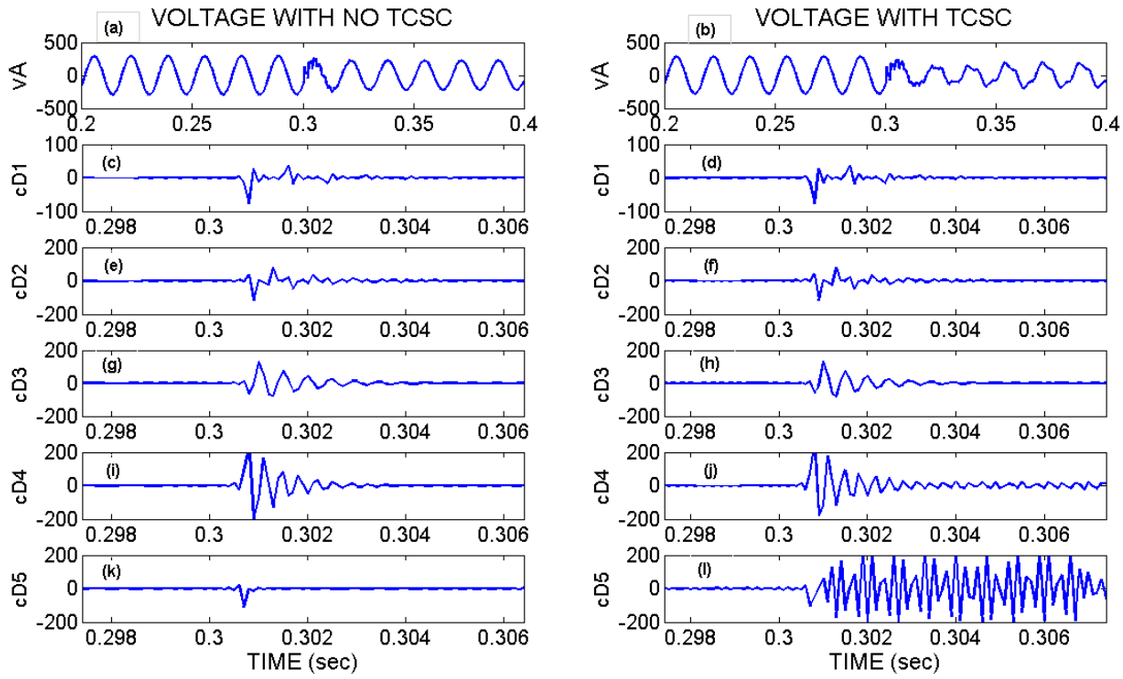

Fig. 19. Detail coefficients obtained in pre-fault and faulted conditions, with and with no TCSC

As can be notice from 19(k) and 19(l), the TCSC effects due the harmonics are detected with cD_5. On the other hand, from 19(c) and (d) the high-frequency traveling waves resulted from the fault are correctly detected with cD_1, regardless of whether or not connected FACTS. Here therefore if lower levels of cDn are used then the harmonics due to TCSC can be discriminated from the mix of signal from the line and fault occurrence.

As a second example, the harmonics injected by the SSSC are also detected with the wavelet transform, because these, it is necessary to separate this signals from those resulted from the fault. In this example, a 6 pulses SSSC is used, so the main harmonic components are 3th, 5th and 7th, which are present at 180 to 420 Hz (Sen, 1998). From table 2, this signal can be analyzed with cD_4 and cD_5, because have a range of 156 to 625 Hz.

To show that harmonics due to SSSC can be discriminated from signals due to fault, a three phase to ground fault is simulated again at 300 km from M_1, as illustrated in fig. 20. The fault occurs at 0.3 s. Two cases are considered: a) without SSSC and b) with SSSC.

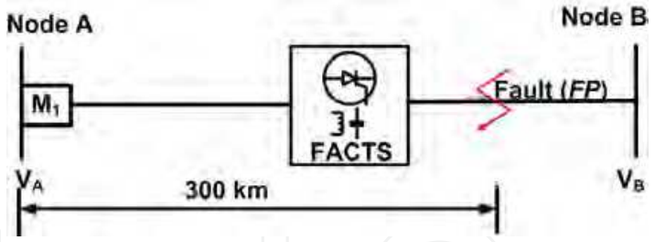

Fig. 20. Three phase to ground fault at 300 km.

As expected, the harmonics due to controller are present with cD_4 and cD_5 as shown in figs. 21(i) to 21 (l). As the same of TCSC case, cD1 can be used to detect the fault signal, with or without the SSSC installed (fig. 21(c) and 21(d)).

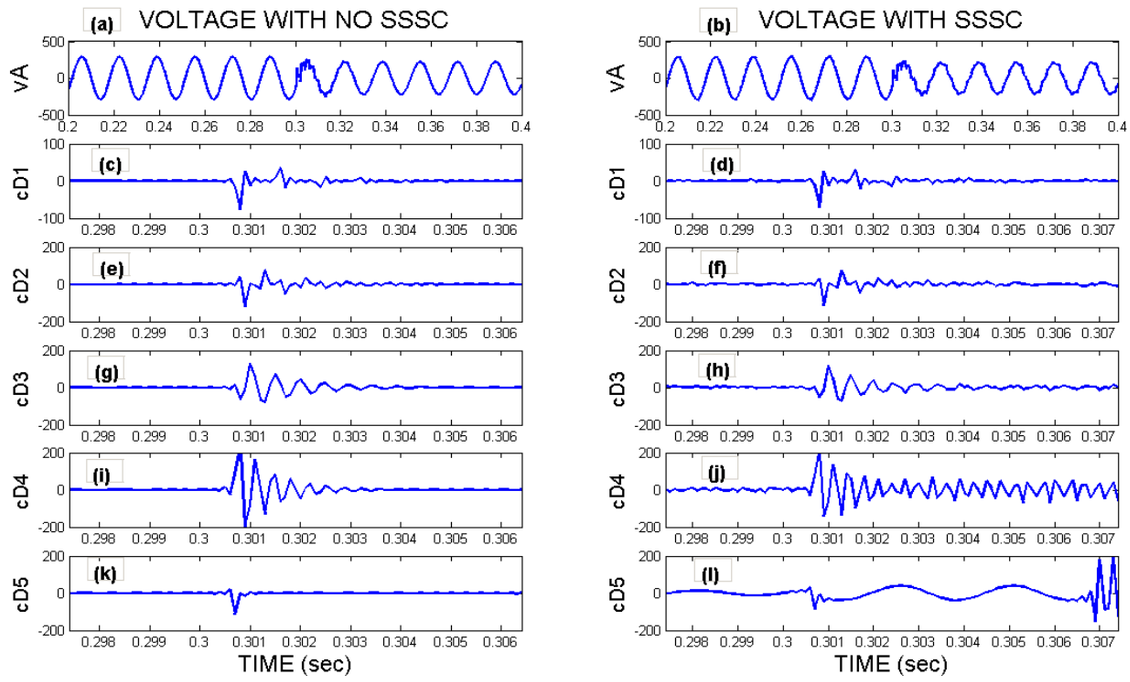

Fig. 21. Coefficients of Detail obtained before and after a fault, with and with no SSSC

As figures 19 and 21 illustrates, the harmonics produced by the FACTS (TCSC and SSSC) are present in levels cD_4 and cD_5. If only lower coefficients of details are considered, then there is no difference between waveforms of voltage/current signals of the faulted line with or without the presence of a FACTS controller. Here therefore cD_1 is a good option for detecting, locating and classifying faults

4.3 Algorithm to detect and locate faults

The algorithm presented in this subsection is based on utilizing traveling waves as mentioned at the beginning of section 4, by means of getting DWT: a) Based on subsection 4.1, the magnitude of traveling wave it's not affected when FACTS lies in its path from fault

position (*FP*) to measurement point (M_1); b) Based on subsection 4.2, harmonics due to FACTS don't affect the measurement of traveling wave at M_1, when cD_1 is selected.

Wavelet toolbox from MATLAB is the tool used to calculate detail coefficients and the distance to the fault location. Figure 22 shows the procedure to extract cD_1 obtained of signals from M_1.

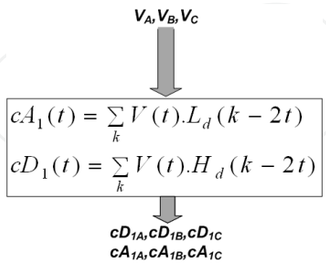

Fig. 22. Procedure to extract the Coefficients of Details

When the voltage signal from M_1 is decomposed in cA_1 and cD_1, cD_1 is used to determinate the instant at which the fault occurs, because of the correspondence with high frequency signals. Figure 23 shows the procedure for analyzing the signals obtained in PSCAD, to detect and locate the fault.

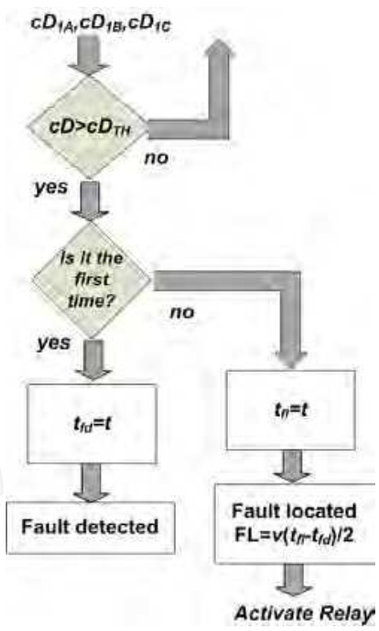

Fig. 23. Procedure to detect and locate fault

Protection relay located at M_1 is continuously monitoring the instant value of voltages V_A, V_B and V_C, in this way, cD_1 is being monitored. If fault is not present, then the only signal monitored by M_1 is the fundamental signal of 60 Hz, as shown in fig. 24 (a). In this case, cD_1 has insignificant values, because there are not signals of frequency determined by this coefficient (2.5 to 5 kHz). Considering a fault occurs in 0.3 seconds at 240 km away from M_1, as illustrated in fig. 24 (b), the transient signal generated by the fault travels across the

transmission line and reaches the protection relay, the value of cD, exceeds a threshold value (cD_{TH}), because the transitory signal due to fault is situated within the range measured by cD_1, then the system detects the Fault and the value of time of fault is stored ($t_{fd}=t$).

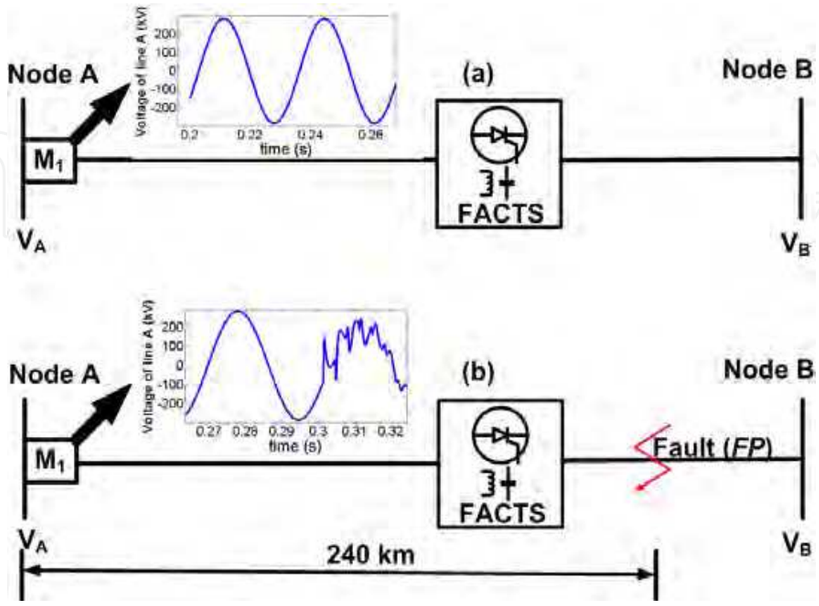

Fig. 24. Signals monitored by M_1, before and after a fault

Once the wave reaches the M_1 position, it is reflected to FP, because the impedance at this point is different to Z_0. Because the impedance of FP is different to Z_0, the wave is reflected again to M_1, as shown in fig. 25.

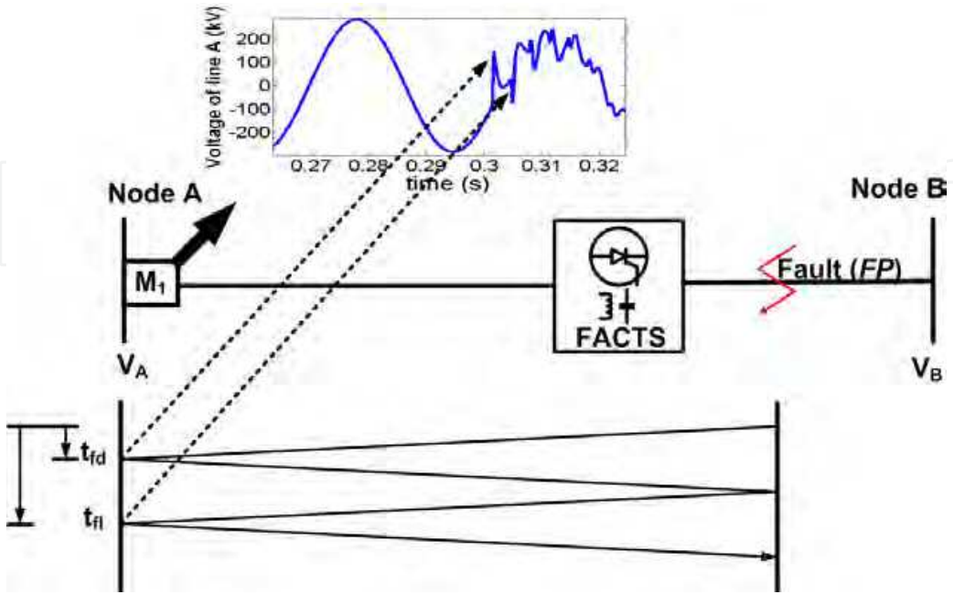

Fig. 25. Path of traveling wave due to fault

When the traveling wave reaches M_1, in a second time, this generates a new peak in cD_1 that uses (13) to locate the distance (FL) at which the fault occurs.

$$FL = \frac{v(t_{fl} - t_{fd})}{2} \tag{13}$$

where v=300,000 (km/s) speed of light, t_{fl} = time of second traveling (s) detection and t_{fd} = time of first traveling detection (s)

5. System under study

To demonstrate the correct operation of procedure presented in section 4, an electrical grid was designed in PSCAD. To validate the detection process, several faults are simulated; ten different types of fault are considered.

To corroborate the location process, fault at every 60 km from M_1 are presented. Figure 26 shows the power grid used for the study cases.

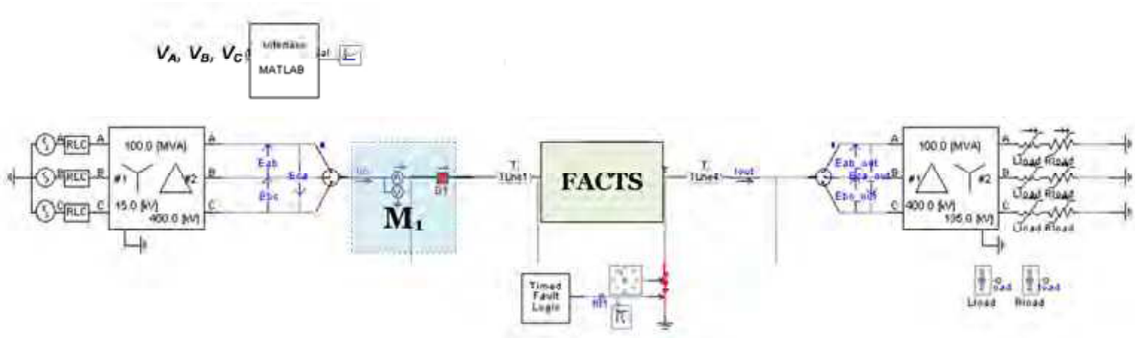

Fig. 26. Electrical grid with series FACTS

cD_1 is used to detect and locate fault. The voltage data (V_A, V_B and V_C) are taken from M_1. These values are fed to MATLAB through an interface. MATLAB performs the tasks presented in subsection 4.3.

After the fault is located a signal of relay activation is sent from MATLAB to PSCAD and protection relay is activated. Protection relay is identified as *B1* in fig. 26 and is located at the same position of M_1.

Electrical parameter of the transmission line are: line voltage: 400 kV; line length: 360 km.; Z_0: 550 Ω, others parameters to adjust TCSC were presented in table 1.

Figures 27 and 28 illustrate the SSSC and TCSC utilized in the case study.

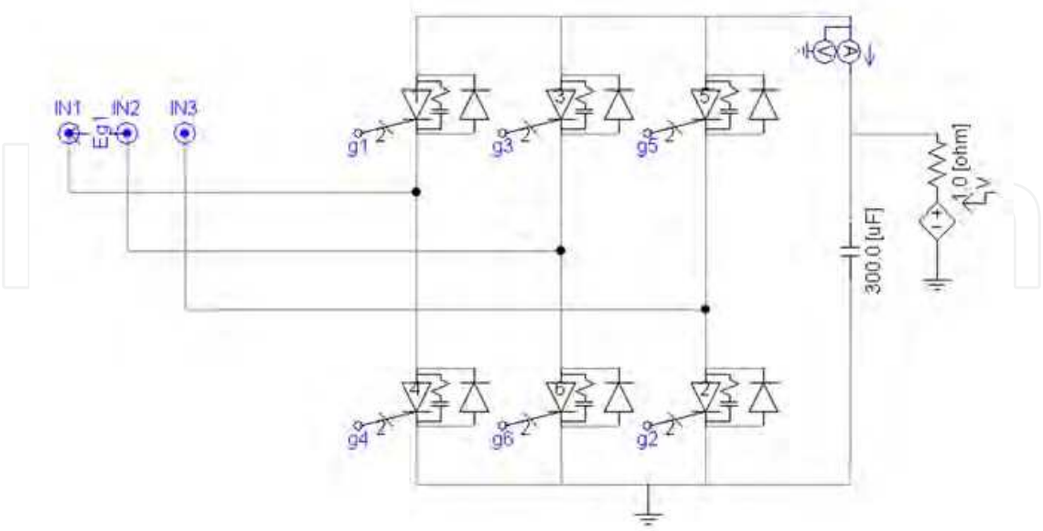

Fig. 27. SSSC configuration for the case study

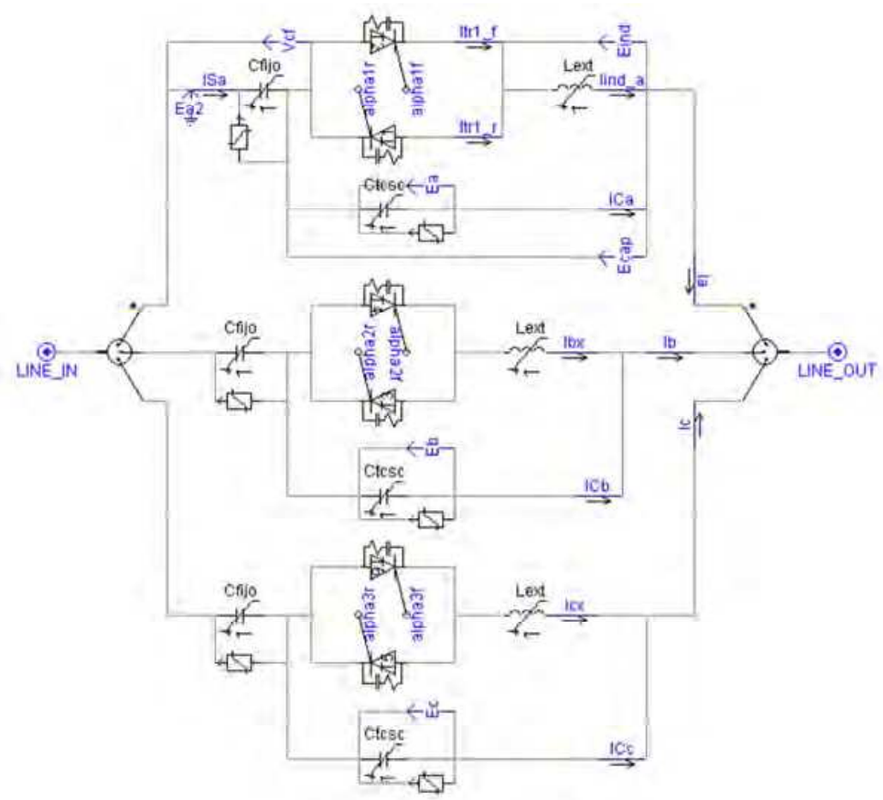

Fig. 28. TCSC configuration for the case study

6. Results

As presented in section 4, traveling waves were no significantly affected by presence of FACTS if cD_1 is selected. Following the procedure showed in section 4, cD_{1A}, cD_{1B}, cD_{1C}, were employed to detect and locate faults. Ten different types of fault were considered to simulation:

1. AG (Phase A to Ground)
2. BG (Phase B to Ground)
3. CG (Phase C to Ground)
4. ABG (Phases A and B to Ground)
5. ACG (Phases A and C to Ground)
6. BCG (Phases B and C to Ground)
7. ABCG (Three Phase Fault to Ground)
8. AB (Phase A to phase B)
9. AC (Phase A to phase B)
10. BC (Phase A to phase B)

Figure 29 shows cD_1 obtained for a fault of type *ABCG* at 240 km from M_1 and t = 0.3 s. As can be notice, cD_{1A}, cD_{1B}, and cD_{1C} appear at 0.3008 s. In this way the fault event can be detected with any cD_1. The magnitude differences among cD_{1A}, cD_{1B}, and cD_{1C} is endorsed to the inception angle of fault, i.e. the value of $V_A(tx)$, $V_B(tx)$ or $V_C(tx)$ (tx represents de instant value when fault occurs) at the moment of fault is incepted. It is important to see that wave requires 0.0008 s to travel from *FP* to M_1. This is the reason for the delay of time in which cD_1 appears and fault is detected. This delay time is considered in detecting time and locating distance.

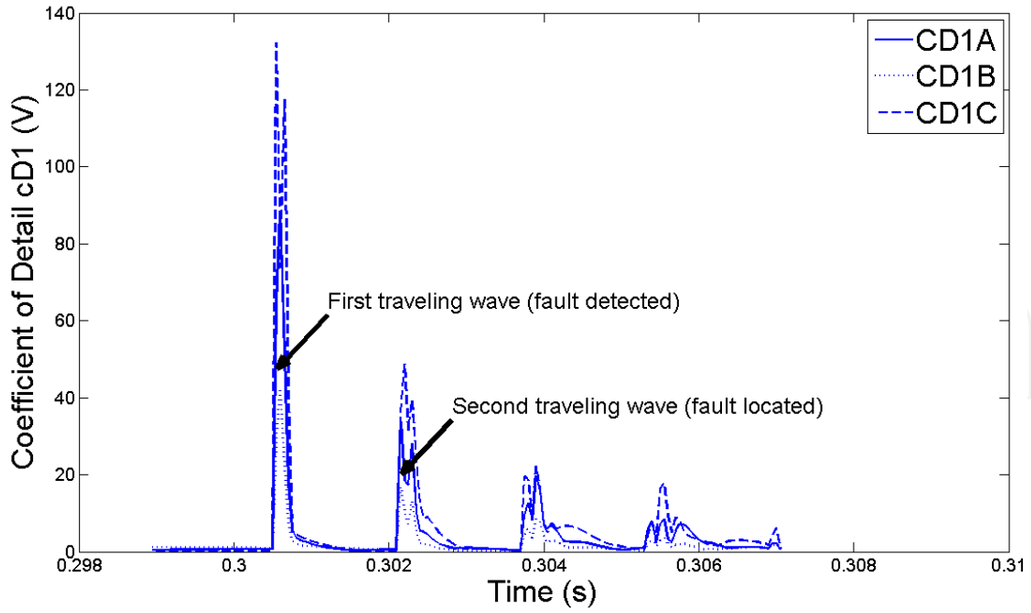

Fig. 29. cD_1 from the three phase fault at t= 0.3 s.

The time elapsed between first and second traveling wave is used by the algorithm to locate the fault. The algorithm developed to detect the fault gives as a result that fault is detected

at 0.3 s and is located at 240 km. These is obtained using (13), in this case, time elapsed between the first and second traveling waves is t_{fl}-t_{fd} = 1.6 ms, so

$$FL = \frac{v(t_{fl} - t_{fd})}{2} = \frac{300000km/s(0.0016s)}{2} = 240km$$

To further test the performance of the developed algorithms, the capability for determining the distance to the fault is also evaluated for different distances. Fig. 30 illustrates that transmission line is divided in 60 km segments. In this way, 6 different positions of fault can be analyzed. As example, the fault is simulated in 0.3 s, at 60 km from M_1

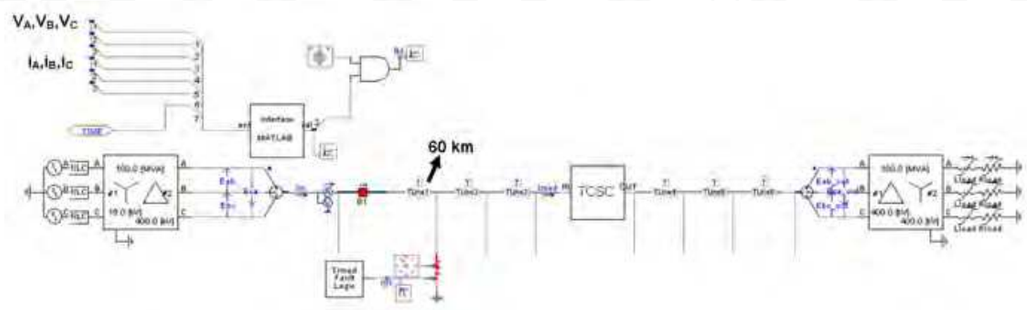

Fig. 30. System used to simulate 6 different locations of faults.

Once the simulation is initiated, voltages values of V_A, V_B and V_C are fed to MATLAB. This latter, develop the algorithm of subsection 4.3 and the result is shown in fig. 31.

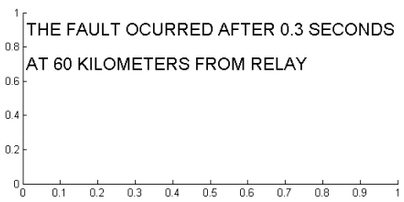

Fig. 31. Result obtained from MATLAB when fault is detected and located

As a resume, the results for 6 different distances to M_1 are shown in tables 3 and 4 for a grid with one FACTS.

TYPE OF FAULT										
Distance (km) to M_1	AG	BG	CG	ABG	BCG	ACG	ABCG	AB	BC	AC
60	60	60	60	60	60	60	60	60	60	60
120	120	120	120	120	120	120	120	120	120	120
180	180	180	180	180	180	180	180	180	180	180
240	240	240	240	240	240	240	240	240	240	240
300	300	300	300	300	300	300	300	292.5	300	300
360	360	360	360	360	360	360	360	360	360	360

Table 3. Distance to the fault for four types of faults in transmission line with TCSC

TYPE OF FAULT										
Distance (km) to M_1	AG	BG	CG	ABG	BCG	ACG	ABCG	AB	BC	AC
60	60	60	60	60	60	60	60	60	60	60
120	120	120	120	120	120	120	120	120	120	120
180	180	180	180	180	180	180	180	180	180	180
240	240	240	240	240	240	240	240	240	240	240
300	300	300	300	300	300	300	300	292.5	300	300
360	360	360	360	360	360	360	360	360	360	360

Table 4. Distance to the fault for four types of faults in transmission line with SSSC

Tables 3 and 4, show that the algorithm closely determines de distance to the fault. For instance, table 3, illustrates that for faults simulated at 60 km from M_1, the distance at which the fault occurs is correctly identified for all types of faults. This is true for cases when TCSC or SSSC is installed at the middle of the line. The distance to fault is well calculated for 60, 120, 180, 240 and 360 km. The only cases in which the algorithm presents deviations are with AB fault type; these have been linked to those faults with a small inception angle (less than 5 degrees). Fig. 32 shows that transient signal (enclosed in red) generated by fault of type AB at 0.3 s is small, in this condition, it's difficult to calculate efficiently the distance to fault.

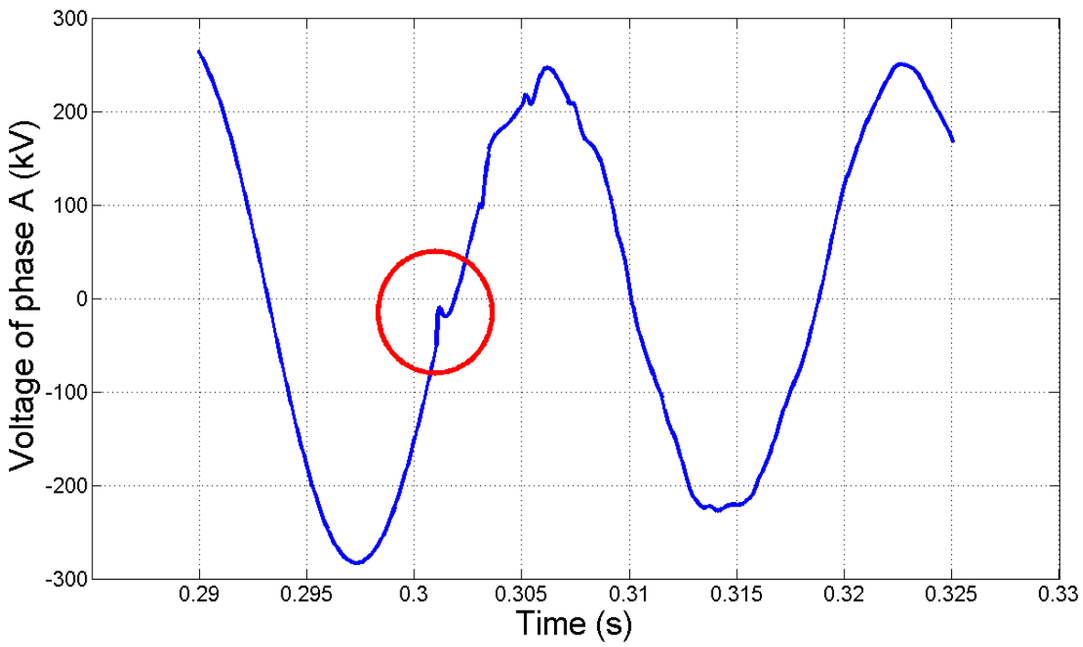

Fig. 32. Voltage of phase A, before and after to AB fault

When the fault is simulated at different time, for example 0.31 s, the fault is correctly detected and located. Fig. 33, shows the screen displayed by MATLAB, after the fault is located.

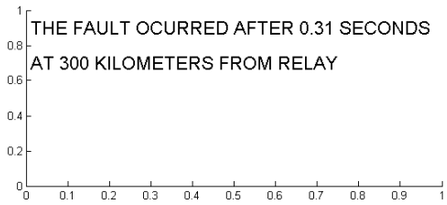

Fig. 33. Screen displayed after *AB* fault, in 0.31 s at 300 km from M_1

The relationship of the time elapsed between first and second traveling waves (t_{elap}=t_{fl}-t_{fd}), has a linear relationship with the distance of fault, this is illustrated in fig 34. This is true when FACTS are or not connected. As this way, the method to calculate de distance to fault using t_{elap} is a better choice compared with distance to fault obtained by measurement of impedance used in conventional schemes. The relationship between distance to fault and impedance are non linear when FACTS is connected (see fig. 10), while using t_{elap}, the distance to fault is easily obtained with (13).

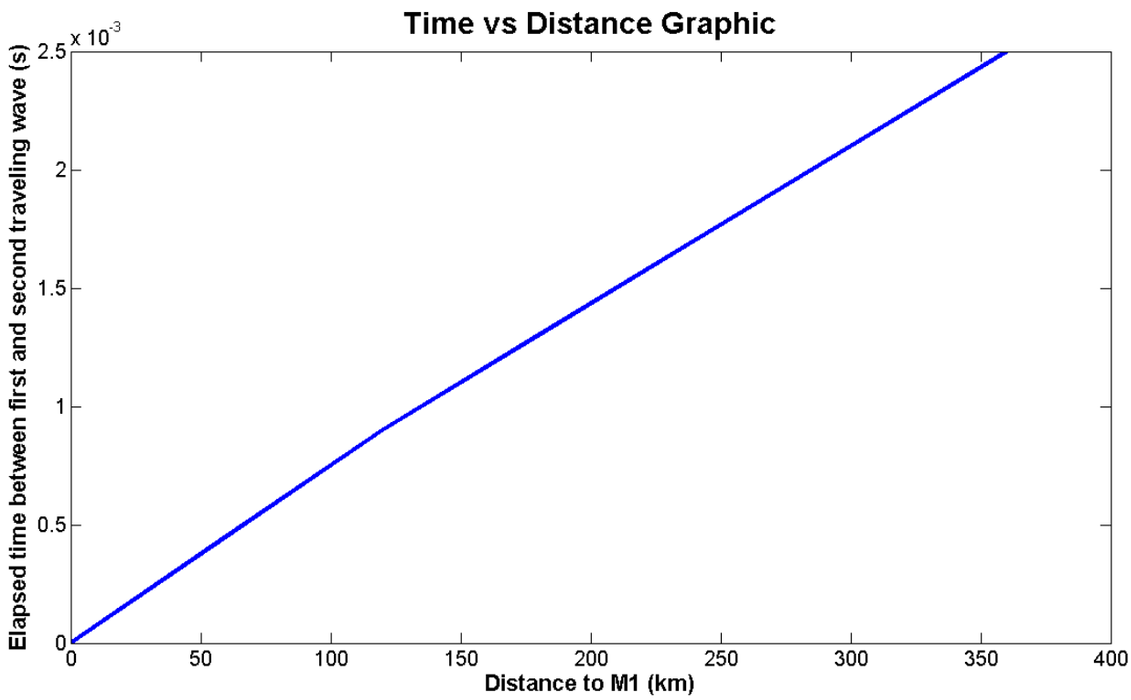

Fig. 34. Relationship between time of traveling waves and distance to fault.

As mentioned earlier, after the detection and location of fault, MATLAB display a screen that includes time of detection and location of fault. After that, MATLAB send an activation signal to protection relay. Fig. 35 shows the line current signals and cD_1, obtained before and after a fault occurs in t=0.3 s at 240 km from M_1

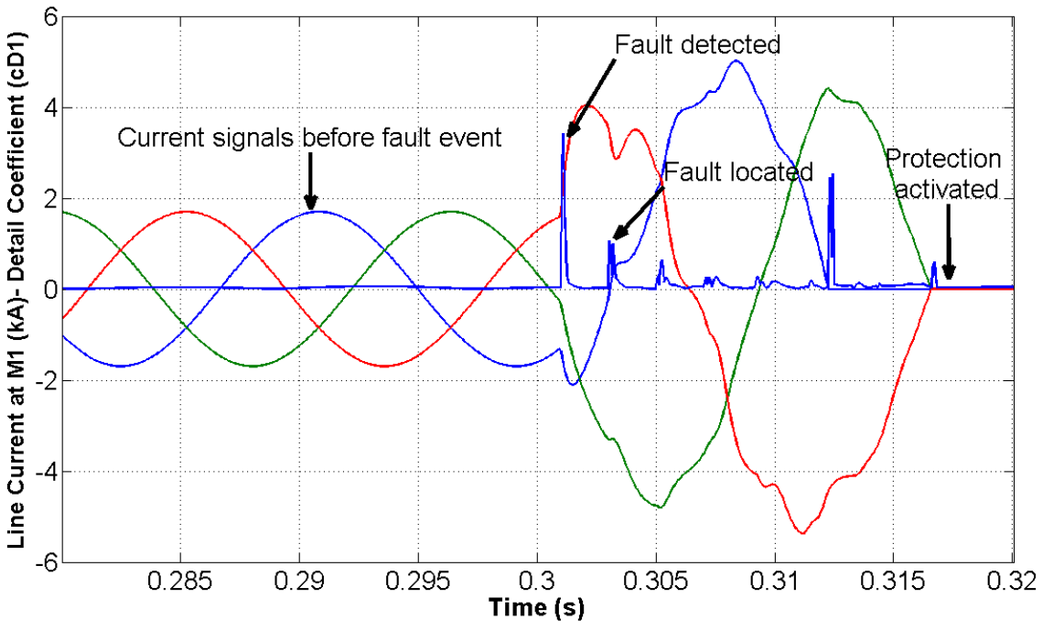

Fig. 35. Protection tripping

As can be seen in fig. 35, before t=0.3 s, the current signals are only the fundamental of 60 Hz. At t=0.3008 s, the algorithm detects the fault event (the wave needs 0.0008 s to reach the M_1 position). The second traveling wave appear at t= 0.3012, at this moment the fault is located. After successful detection and locating of the fault event the protection is activated. The time given to activating relay is sufficiently small (15 ms after detection of fault) to don't compromise coordination with others protection relays.

7. References

Chen Y, et. al. (2010), "Short-Term Load Forecasting: Similar Day-Based Wavelet Neural Networks", *IEEE Transactions on Power Systems, Vol. 25, No. 1*, pp. 322-330, Feb. 2010

Chia-Hung L. & Chia-Hao W. (2006), "Adaptive Wavelet Networks for Power-Quality Detection and Discrimination in a Power System", *IEEE Transactions on Power Delivery, Vol. 21, No. 3*, pp. 1106-111, July 2006

Daneshpooy A.&Gole A.M. (2001), "Frequency Response of the Thyristor Controlled Series Capacitor", *IEEE Transactions on Power Delivery, Vol. 16, No. 1*, pp. 53-58, Jan 2001

Hingorani N. & Gyugyi L. (2000), *Understanding FACTS*, IEEE PRESS, New York USA, 2000

Kashyap K.H. & Shenoy U.J. (2003), "Classification Of Power System Faults Using Wavelet Transforms And Probabilistic Neural Networks", *Proceedings of the 2003 International Symposium on Circuits and Systems*, May 2003, pp 423-426

Kazemi A., Jamali S. & Shateri H. (2005), "Effects of STATCOM on Distance Relay". In *Proc. 2005, IEEE Transmission and Distribution Conference and Exposition*, pp. 1-6

Khederzadeh M. (2008), "UPFC Operating Characteristics Impact on Transmission Line Distance Protection", In *Proc. 2008, IEEE-PES General Meeting - Conversion and Delivery of Electrical Energy in the 21st Century*, pp. 1-6

Misiti M., Oppenheim & Poggi J. M. (2001), "Wavelet Toolbox Users Guide", *The Math Work, Inc.*, 2001

Ning J. & Gao W. (2009), "A wavelet-based method to extract frequency feature for power system fault/event analysis", *Power & Energy Society General Meeting*, IEEE, Calgary, AB, Oct. 2009.

Pourahmadi-Nakhli M. & Safavi A. (2011), "Path Characteristic Frequency-Based Fault Locating in Radial Distribution Systems Using Wavelets and Neural Networks", *IEEE Trans. on Power Delivery*, vol. 26, pp. 772-781, Apr. 2011.

Sen K.K. (1998), "SSSC - Static Synchronous Series Compensator: Theory, Modeling, and Applications", *IEEE Trans. on Power Delivery*, vol. 13, pp. 241-246, Jan. 1998

Shehab-Eldin E.H. & McLaren P.G. (1988), "Travelling wave distance protection - problem areas and solutions", *IEEE Trans. on Power Delivery,* Vol. 3, No. 3, pp. 894-902, Jul. 1988

Tse N.C.F (2006), "Practical application of wavelet to power quality analysis", *Power Engineering Society General Meeting*, IEEE, Montreal, Que, Oct. 2006.

Zhou X.Y, Wang H.F., Aggarwal R.K. & Beaumont P. (2005), "The Impact of STATCOM on Distance Relay", In *Proc. 2005, Power Systems Computation Conference*, pp. 1-7

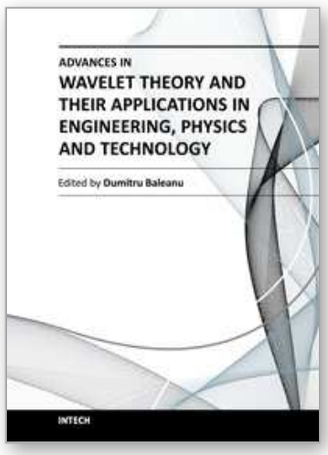

Advances in Wavelet Theory and Their Applications in Engineering, Physics and Technology

Edited by Dr. Dumitru Baleanu

ISBN 978-953-51-0494-0
Hard cover, 634 pages
Publisher InTech
Published online 04, April, 2012
Published in print edition April, 2012

The use of the wavelet transform to analyze the behaviour of the complex systems from various fields started to be widely recognized and applied successfully during the last few decades. In this book some advances in wavelet theory and their applications in engineering, physics and technology are presented. The applications were carefully selected and grouped in five main sections - Signal Processing, Electrical Systems, Fault Diagnosis and Monitoring, Image Processing and Applications in Engineering. One of the key features of this book is that the wavelet concepts have been described from a point of view that is familiar to researchers from various branches of science and engineering. The content of the book is accessible to a large number of readers.

INTECH
open science | open minds

InTech Europe
University Campus STeP Ri
Slavka Krautzeka 83/A
51000 Rijeka, Croatia
Phone: +385 (51) 770 447
Fax: +385 (51) 686 166
www.intechopen.com

InTech China
Unit 405, Office Block, Hotel Equatorial Shanghai
No.65, Yan An Road (West), Shanghai, 200040, China
中国上海市延安西路65号上海国际贵都大饭店办公楼405单元
Phone: +86-21-62489820
Fax: +86-21-62489821

IntechOpen